Lithos 344–345 (2019) 207–216

Contents lists available at ScienceDirect

Lithos

journal homepage: www.elsevier.com/locate/lithos

Minor elements in olivine inspect the petrogenesis of orogenic peridotites

Bin Su [a], Yi Chen [a,b,c,*], Qian Mao [a], Di Zhang [a], Li-Hui Jia [a], Shun Guo [a,b]

[a] State Key Laboratory of Lithospheric Evolution, and Institutions of Earth Science, Institute of Geology and Geophysics, Chinese Academy of Sciences, Beijing 100029, China
[b] Chinese Academy of Sciences Center for Excellence in Tibetan Plateau Earth Sciences, Beijing 100101, China
[c] University of Chinese Academy of Sciences, Beijing 100049, China

ARTICLE INFO

Article history:
Received 1 May 2019
Received in revised form 26 June 2019
Accepted 26 June 2019
Available online 29 June 2019

Keywords:
Olivine
Minor element
Orogenic peridotite
Metasomatism
Subduction zone

ABSTRACT

A large dataset of minor elements (Ni, Mn, Co, Zn, Ca, Ti, Al, Cr and Na) in olivines from orogenic peridotites is reported to investigate the application of these elements as sensitive tracers of mantle processes in subduction zones. Orogenic mantle peridotites can be distinguished from crustal peridotites by overall higher Ni and lower Co and Zn contents in olivine. In particular, the Ni/Co ratio of olivine can successfully discriminate between the two types of peridotites. When mantle peridotites underwent transfer from hot lithospheric mantle to cool subduction zones, olivine Ca, Al and Cr contents dramatically decreased, and Ca in olivine can be a useful geothermometer for orogenic peridotites. The Na contents of olivines from garnet-facies mantle peridotites (mostly >20 ppm) are typically higher than those from spinel-facies mantle peridotites (mostly <11 ppm), indicating that Na in olivine is a potential pressure indicator for orogenic peridotites. The high Ti contents of olivine may be caused by subducted crustal metasomatism, producing the wide occurrence of Ti-clinohumite and rutile in strongly metasomatized garnet lherzolites. Olivines from these high-Ti garnet lherzolites also have Mn contents deviating from the normal mantle olivine range, implying high sensitivity of Mn in olivine to crust–mantle interaction in subduction zones. Our data highlight the broad prospects for olivine geochemistry in the realm of subduction zone geodynamics.

1. Introduction

Mantle fragments occur tectonically within many high-pressure (HP) and ultrahigh-pressure (UHP) metamorphic terranes along collisional margins. These fragments crop out as blocks or lenses in metamorphosed continental crust rocks and are named 'orogenic peridotites', 'peridotite massifs' or 'alpine-type peridotites' (Brueckner and Medaris, 2000; Zhang et al., 2000). Most orogenic peridotites originated from the mantle wedge and were then incorporated into the subduction channel at various depths (30–200 km) (Yang and Jahn, 2000; Ye et al., 2009; Zhang et al., 2009). These peridotites can thus provide important insight into processes in both deep subduction zones and the upper mantle (Bodinier and Godard, 2003; Zheng et al., 2014). Compared with small-sized mantle xenoliths in volcanic rocks, orogenic peridotites range from 1 m^2 to >100 km^2 in size and allow evaluation of rock-type relationships and the scale of mantle heterogeneities (Beyer et al., 2006; Chen et al., 2013a; Song et al., 2007). Therefore, orogenic peridotites are also a significant complement to mantle xenoliths for understanding the composition and evolution of the Earth's mantle (Lenoir et al., 2001; Spengler et al., 2006). More importantly, orogenic peridotites and surrounding supracrustal rocks can be viewed as a slab–mantle wedge interface, which makes orogenic peridotites a natural window into crust–mantle interaction in subduction zones (Chen et al., 2013b; Malaspina et al., 2006; Scambelluri et al., 2008; Zheng, 2012).

Olivine is the most abundant mineral in peridotite and has an exclusive status in our understanding of the Earth's mantle (De Hoog et al., 2010; Foley et al., 2013; Hervig et al., 1986). Despite its simple major element compositions, olivine contains a number of petrogenetically significant minor elements, such as Ni, Mn, Co, Zn, Ca, Ti, Al, Cr and Na, mostly below 0.1 wt% of oxide except for NiO (Prelević et al., 2013; Sobolev et al., 2009). In general, compatible (Ni, Co and Zn) and mildly incompatible elements (Mn) in olivine can shed light on mantle melting processes (e.g., O'Reilly et al., 1997; Simkin and Smith, 1970; Xu et al., 2010), as well as the sources of primitive mantle-derived magmas (e.g., Sobolev et al., 2005, 2007; Straub et al., 2008). The temperature dependence of Ca, Al and Cr contents in olivine has been recognized in experiments and natural rocks (Bussweiler et al., 2017; Coogan et al., 2014; De Hoog et al., 2010). Taura et al. (1998) demonstrated that the partition coefficient of Na between olivine and melt increases with pressure up to 14 GPa. Moreover, a few elements (e.g., Ti and Zn) have been

* Corresponding author at: State Key Laboratory of Lithospheric Evolution, and Institutions of Earth Science, Institute of Geology and Geophysics, Chinese Academy of Sciences, Beijing 100029, China.
E-mail address: chenyi@mail.iggcas.ac.cn (Y. Chen).

https://doi.org/10.1016/j.lithos.2019.06.029
0024-4937/

used as tracers for mantle metasomatism (Foley et al., 2006; Prelević et al., 2013; Su et al., 2016a). Consequently, minor elements in olivine have become powerful tools to unravel the nature and processes of the mantle. However, the minor element abundances of orogenic peridotite olivines have received much less attention than those of mantle and igneous olivines, which hampers our understanding of the mantle geodynamics in subduction zones.

In this study, we selected forty-one orogenic peridotite samples mainly from the Dabie–Sulu UHP metamorphic terrane in eastern China, with the rest from the Western Gneiss Region (WGR) in western Norway, the South Altyn Tagh in western China and the Seve Nappe Complex (SNC) in Sweden (Fig. 1). We carried out major and minor element analyses on olivines from these samples using a high-precision electron probe microanalyzer (HP-EPMA). A comparison of minor elements in olivines from orogenic peridotites with those from continental lithospheric mantle peridotites can help us better understand the origin and evolution of orogenic peridotites.

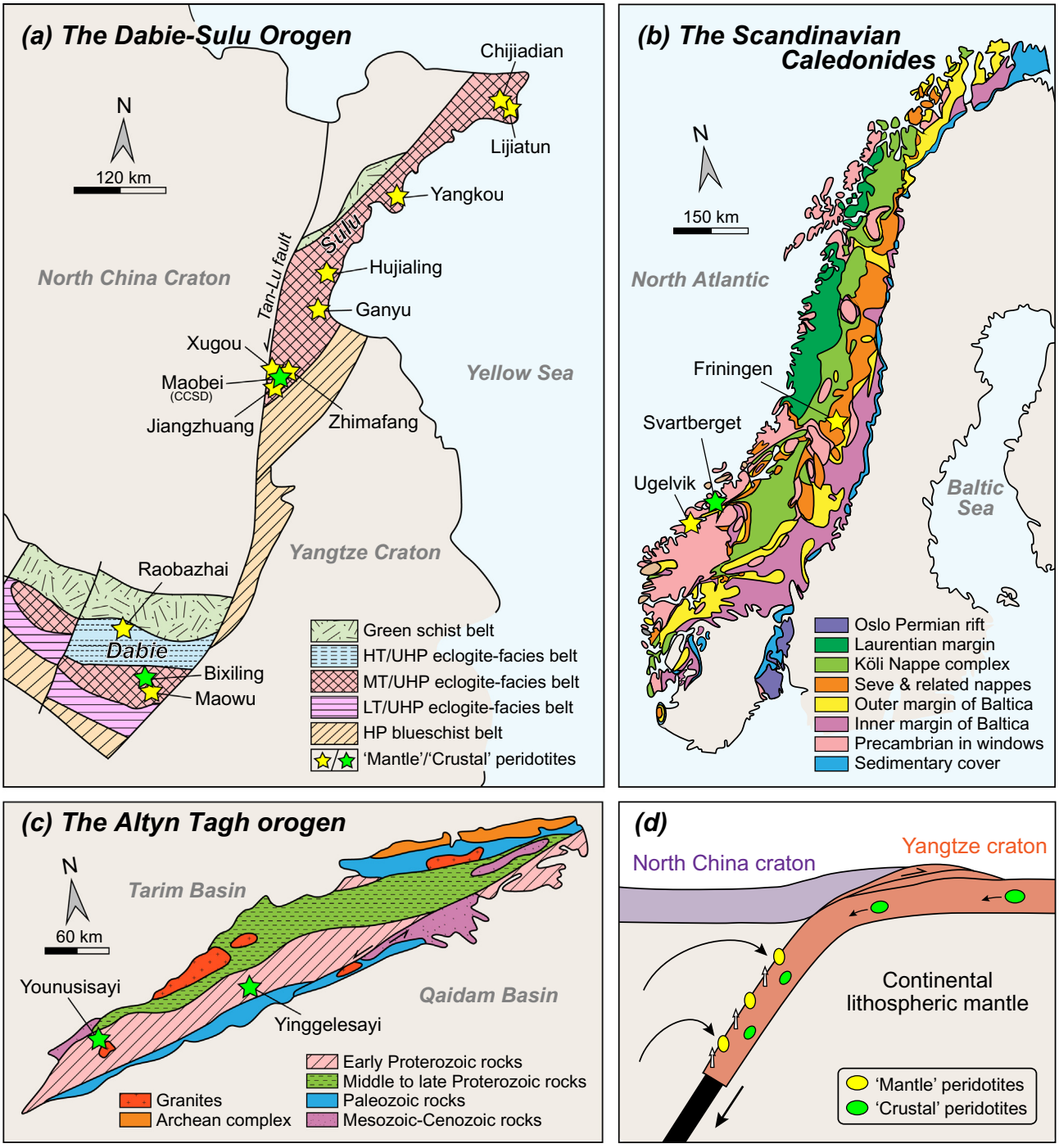

Fig. 1. Locations of orogenic peridotites collected in this study on geological maps of (a) the Dabie–Sulu orogen (after Zhang et al., 2009), (b) the Scandinavian Caledonides (after Gee et al., 2013) and (c) the Altyn Tagh orogen (after Liu et al., 2002). (d) A schematic model for the interpretive dual origin (mantle and crustal) of orogenic peridotites after Zhang et al. (2000).

2. Samples

The collected orogenic peridotites consisted of 23 samples from the Sulu orogen (9 locations), 11 samples from the Dabie orogen (3 locations), 3 samples from the WGR (2 locations), 2 samples from the South Altyn Tagh (2 locations) and 2 samples from the SNC (1 location). The occurrences of coesite and/or diamond in crustal rocks (mostly gneisses and eclogites) provide direct evidence for UHP metamorphism of these orogenic terranes as a consequence of deep continental subduction (e.g., Gai et al., 2017; Smith, 1984; Xu et al., 1992; Ye et al., 2000). The studied peridotites comprise lherzolites, harzburgites and dunites. They represent either mantle wedge slices (Fig. 1d), such as those from Zhimafang, Maowu and Ugelvik (Chen et al., 2017; Spengler et al., 2006; Ye et al., 2009) or crustal mafic–ultramafic cumulates, such as those from Bixiling, Maobei and Svartberget (Li et al., 2011; Vrijmoed et al., 2013; Zheng et al., 2008). The majority of the studied samples are garnet-facies peridotites (31 samples), which refer to garnet peridotites with or without minor spinel. The remaining 10 samples are spinel peridotites with or without very rare garnet. Details about sample locations, lithologies and origins are listed in Table 1. The peak metamorphic temperatures of these peridotites fall within the narrow range of 700–900 °C, but their peak pressures show a broad range from ~2 to 7 GPa (e.g., Chen et al., 2013a; Liu et al., 2002; van Roermund and Drury, 1998; Yang and Jahn, 2000). Furthermore, several garnet lherzolite samples from Zhimafang, Jiangzhuang, Chijiadian and Yangkou contain various secondary phases (e.g., phlogopite, Ti-clinohumite, zircon, pargasite and magnesite), indicating that they have been metasomatized by slab-derived liquids. In contrast, dunites/harzburgites from Raobazhai, Maowu and Ugelvik are relatively lack of secondary metasomatic minerals.

3. Method and results

Olivines from orogenic peridotites were analyzed for Si, Mg, Fe, Ni, Mn, Co, Zn, Ca, Ti, Al, Cr and Na with a Cameca SXFive EPMA at the Institute of Geology and Geophysics, Chinese Academy of Sciences (IGGCAS). The analytical conditions were a 25 kV acceleration voltage and a 900 nA beam current for minor elements (Ni, Mn, Co, Zn, Ca, Ti, Al, Cr and Na) and 25 kV, 40 nA for major elements (Si, Mg and Fe) with a 5 μm diameter. The major and minor elements were acquired using five analyzing crystals as follows: two TAP for Si, Mg, Na and Al (Kα); one LIF for Fe, Cr and Co (Kα); one LPET for Ca and Ti (Kα); and one LLIF for Mn, Ni and Zn (Kα). Sodium was measured immediately after major elements to minimize its possible loss during analysis. The

Table 1
The average compositions of major and minor elements in olivines from orogenic peridotites.

Locality	Sample No.	Lithology	Mg	Fe	Si	Na	Cr	Co	Ca	Ti	Mn	Ni	Zn	Al	Fo	Ni/Co
			wt%			ppm										
Orogenic 'mantle' peridotites																
Chijiadian, Sulu	CJD9	Grt-L	29.33	7.71	19.01	28	<16	147	42	93	1156	3191	13	12	89.74	21.7
	CJD4	Grt-L	30.06	6.98	18.94	40	16	149	42	92	674	3035	39	15	90.82	20.4
	CH17	Grt-L	29.63	7.54	18.89	28	<16	141	42	93	1021	3285	<13	<7	90.03	23.3
Lijiatun, Sulu	12LJT8	Spl-D	30.54	5.85	19.65	12	<16	141	28	26	818	3127	35	<7	92.30	22.2
	12LJT9	Spl-D	30.56	5.83	19.80	<11	<16	140	35	38	815	3119	40	<7	92.33	22.3
Yangkou, Sulu	YK3	Grt-L	30.10	7.25	19.18	33	25	153	17	53	664	2812	31	<7	90.51	18.4
	YK4	Grt-L	30.34	6.61	19.14	22	<16	141	13	59	730	3112	28	<7	91.34	22.1
Hujialing, Sulu	HJL23	Grt-D	30.98	5.70	19.22	28	<16	141	14	54	474	3316	52	<7	92.58	23.4
	RH004	Spl-H	30.79	6.11	19.22	11	<16	135	27	48	833	3136	31	<7	92.05	23.3
	RH04	Spl-H	30.67	6.13	19.19	<11	<16	133	46	48	854	3108	33	<7	92.00	23.4
Ganyu, Sulu	14QH28a	Grt-L	29.98	7.52	18.99	60	24	132	47	36	1089	2890	23	10	90.16	21.8
	14QH28b	Grt-L	29.91	7.57	18.79	57	16	131	70	32	1101	2850	29	12	90.08	21.7
Zhimafang, Sulu	00ZMF2	Grt-L	30.64	6.19	19.12	31	<16	140	15	46	711	3102	53	14	91.92	22.2
	00ZMF3	Grt-L	30.69	5.87	19.22	30	<16	150	15	54	523	3178	51	<7	92.31	21.1
	ZMF11c	Grt-L	30.49	5.99	19.30	32	<16	141	11	56	585	3083	54	<7	92.12	21.8
Xugou, Sulu	04XG1	Grt-L	30.48	6.32	19.27	60	16	135	28	69	887	3096	31	23	91.73	22.9
	14XG1a	Grt-L	30.06	6.68	19.26	63	<16	139	32	58	1028	3063	56	11	91.18	22.0
	14XG3	Grt-L	30.57	6.22	19.47	69	<16	135	26	34	927	3107	43	12	91.87	23.0
Jiangzhuang, Sulu	JZ8e	Grt-L	29.88	6.50	19.24	54	<16	148	20	79	580	3285	57	11	91.35	22.2
	JZ9e	Grt-L	30.57	6.49	18.89	39	<16	148	13	79	565	3253	56	8	91.54	21.9
	JZ10b5	Grt-L	29.93	6.23	19.60	59	<16	157	18	72	526	3252	68	7	91.69	20.8
Maowu, Dabie	15 MW2	Grt-H	31.05	5.63	19.07	57	<16	137	11	7	718	3148	39	<7	92.68	23.0
	15 MW1	Spl-D	30.89	5.64	19.20	18	<16	136	22	11	723	3062	38	<7	92.64	22.5
	09 MW40	Spl-D	30.90	5.81	19.00	19	<16	132	6	13	793	2983	37	<7	92.44	22.7
Raobazhai, Dabie	15RBZ3	Spl-D	30.54	5.23	19.32	<11	<16	137	72	53	755	3119	34	<7	93.06	22.8
	15RBZ5	Spl-H	30.79	5.71	19.22	<11	<16	137	74	13	809	3075	29	<7	92.53	22.4
	15RBZ12	Spl-L	29.21	7.45	19.06	<11	<16	157	50	27	1065	2951	34	<7	90.00	18.8
Friningen, SNC	17FR1	Grt-D	31.03	5.63	19.26	23	<16	126	23	15	772	2843	23	<7	92.68	22.5
	17FR4	Grt-D	30.82	5.73	19.05	50	<16	129	62	<5	757	2911	32	7	92.51	22.6
Ugelvik, WGR	17Ug2	Grt-D	30.84	5.45	19.37	38	21	133	66	<5	600	3097	40	<7	92.86	23.2
	17Ug5	Grt-D	30.95	5.42	19.42	26	20	130	65	<5	642	3048	30	8	92.91	23.4
Orogenic 'crustal' peridotites																
Maobei, Sulu	p5a-1	Grt-H	27.13	12.10	18.19	11	<16	208	30	72	970	1870	121	13	83.74	9.0
	p3c	Grt-L	27.62	11.32	18.48	50	<16	182	38	77	836	1733	139	13	84.86	9.5
Bixiling, Dabie	03BXL-2	Grt-L	27.17	10.91	18.66	27	<16	251	32	50	503	1586	261	7	85.13	6.3
	03BXL-5	Grt-L	28.02	9.86	18.59	24	<16	319	27	46	349	3107	265	7	86.72	9.7
	16BXL3	Grt-L	26.95	11.22	18.68	<11	<16	250	15	45	786	1582	240	<7	84.66	6.3
	16BXL6	Grt-L	27.16	11.39	18.46	13	<16	219	18	46	920	1321	196	<7	84.57	6.0
	16BXL7	Grt-L	27.16	11.78	18.77	17	<16	206	18	41	1009	1245	187	<7	84.12	6.0
Yinggelisayi, Altyn	15A-14-3	Grt-L	25.22	15.04	18.19	16	<16	206	68	18	1987	1246	82	<7	79.39	6.1
Younusisayi, Altyn	17A-88-1	Spl-L	28.20	10.61	18.60	79	26	181	90	11	1895	1025	51	8	85.92	5.7
Svartberget, WGR	17SV2	Grt-L	27.08	12.25	18.50	12	22	255	94	46	1510	1672	80	13	83.55	6.5

Note: 1. Grt-L, garnet lherzolite; Grt-H, garnet harzburgite; Grt-D, garnet dunite; Spl-L, spinel lherzolite; Spl-H, spinel harzburgite; Spl-D, spinel dunite.
2. The less-than sign (e.g., <11) indicates the minor element data below the HP-EPMA detection limits.

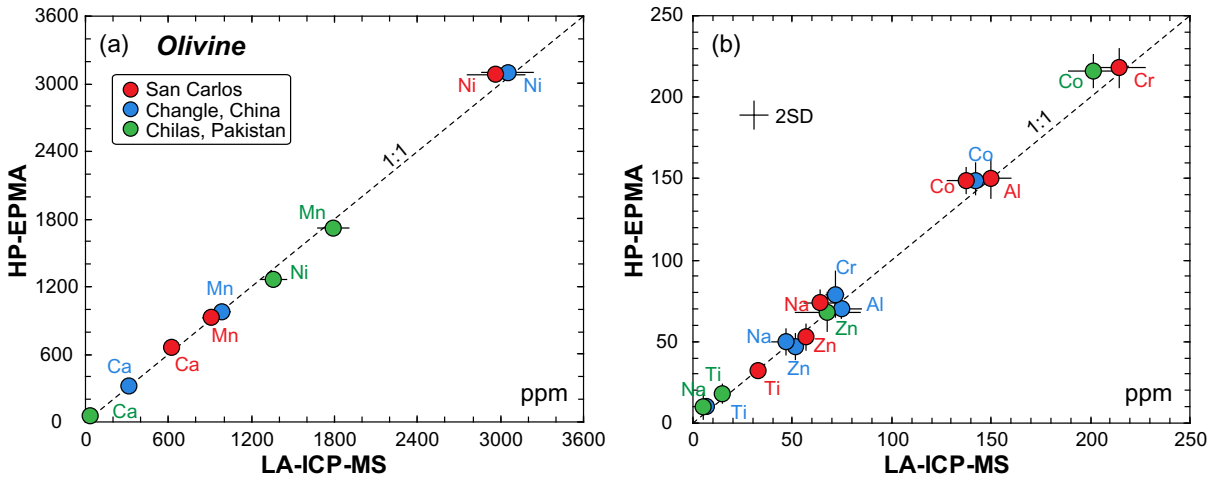

Fig. 2. Comparison of minor element contents in the San Carlos olivine and two nature olivines (Changle and Chilas) obtained by HP-EPMA and LA-ICP-MS.

peak counting times were 20 s for Si, Mg and Fe; 120 s for Na, Cr, Ca, Mn, Ni and Zn; and 240 s for Co, Ti and Al. The San Carlos olivine reference material was analyzed two times per 20–30 measurements to monitor machine drifts. All data were corrected on-line using a modified ZAF (atomic number, X-ray absorption, fluorescence) correction procedure. The accuracy of HP-EPMA was tested by comparing analyses of the San Carlos olivine and two natural olivines from Changle (eastern China) and Chilas (northern Pakistan) measured by laser ablation inductively coupled plasma mass spectrometry (LA-ICP-MS) at the State Key Laboratory of Continental Dynamics (Northwest University). As shown in Fig. 2, all data plot well along the 1:1 correspondence line within the internal precision of both methods. The detection limits are 10 ppm for Ni, 9 ppm for Mn, 14 ppm for Co, 13 ppm for Zn, 5 ppm for Ca, 5 ppm for Ti, 7 ppm for Al, 16 ppm for Cr and 11 ppm for Na, based on a 3σ estimate of the measured background variance. The standard errors are 4–16 ppm (3σ; see supplemental file Table S1 for details).

All measured data consisting of 1976 olivine analyses are listed in supplemental file Table S2. The average values of major and minor elements in measured olivines are summarized in Table 1. All olivines exhibit large compositional variations, with Fo values [atomic 100 × Mg/(Mg + Fe)] from 79.1 to 93.2, Ni contents from 971 to 3498 ppm, Co contents from 114 to 331 ppm, Zn contents from <13 (below detection limit) to 331 ppm, and Mn contents from 327 to 2111 ppm. In contrast, most olivines have relatively restricted Ca (6–98 ppm), Cr (<16–52 ppm), Al (<7–70 ppm), Na (<11–94 ppm) and Ti (5–92 ppm) contents. Approximately half of the analyses have Cr and Al contents below the detection limits of 16 and 7 ppm, respectively. Overall, olivine chemical compositions vary among samples, especially those from different locations, but their variations are relatively insignificant within each sample (40–50 measurements).

4. Discrimination between 'mantle' and 'crustal' origins for orogenic peridotites

As proposed in previous studies (e.g., Brueckner and Medaris, 2000; Carswell et al., 1983; Zhang et al., 2000), orogenic peridotites are commonly grouped into two types (Fig. 1d): (1) 'mantle' peridotite (type A or Mg–Cr-type peridotite) generally derived from the mantle wedge (Beyer et al., 2006; Chen et al., 2017; Su et al., 2016a; Zhang et al., 2000; Zheng et al., 2005) and (2) 'crustal' peridotite (type B or Fe–Ti-type peridotite) produced by the intrusion and crystallization of mantle-derived magmas into the lower crust prior to subduction (Carswell et al., 1983; Liu et al., 2002; Zheng et al., 2008). Distinguishing these two types will help improve our understanding of orogenic processes, mantle evolution and crust–mantle interaction.

Previous work suggested that crustal peridotites show complex compositional layers in the outcrop and well-developed cumulative textures, which were considered to be different from mantle peridotites (Carswell et al., 1983; Medaris and Carswell, 1990). However, many studies have demonstrated that mantle peridotites can exhibit field

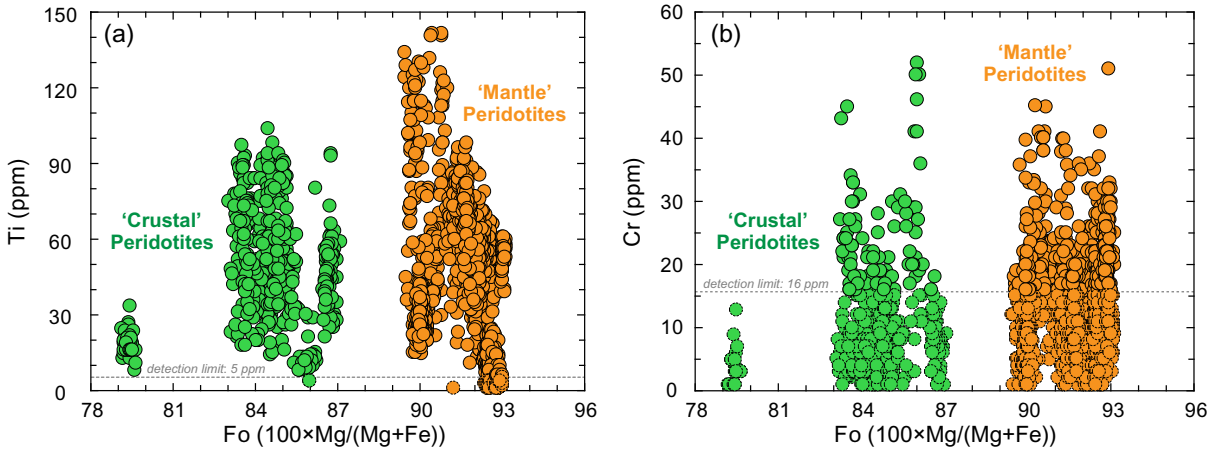

Fig. 3. (a) Ti and (b) Cr contents in olivines from the mantle and crustal orogenic peridotites vs. Fo values. Dashed circles mark the data (Ti or Cr contents) below the detection limits of HP-EPMA.

relationships and petrography similar to those of crustal peridotites [see Chen et al., 2015 for details]. To better distinguish these two types of peridotites, researchers have mainly focused on whole-rock geochemistry (MgO, FeO, Ti, Cr, Ni, Zr, Nb and rare earth elements) (Reverdatto et al., 2008), garnet and clinopyroxene compositions (Zhang et al., 2000), and whole-rock platinum group elements (e.g., Chen et al., 2015). Given that orogenic mantle peridotites have undergone extensive crustal metasomatism, they may possess compositional characteristics of both depleted mantle and subducted crust (Chen et al., 2017; Vrijmoed et al., 2013). Therefore, the whole-rock and mineral (garnet and clinopyroxene) compositions of the two types of peridotites partially overlap (e.g., Ackerman et al., 2009; Chen et al., 2013b), making the above criteria difficult to apply widely.

As a primary mineral in most peridotites, olivine can potentially be used to constrain the origin of orogenic peridotites. In general, olivines in mantle peridotites have higher Fo values (89–94) than those in crustal peridotites (mostly 80–88); however, parts of crustal peridotites (e.g., cumulative dunites) have olivine Fo values (88.5–90.9) similar to those of mantle peridotites (Su et al., 2016b). Carswell et al. (1983) showed that mantle peridotites from the WGR have higher Cr and lower Ti contents than crustal peridotites. However, the Cr and Ti contents in olivines from the two types of peridotites are actually indistinguishable (Fig. 3). Since Ni, Co and Zn are compatible in olivine and relatively robust against metasomatism, they have potential to trace the origins of orogenic peridotites. As shown in Fig. 4, olivines from mantle peridotites exhibit overall higher Ni (2587–3498 ppm vs. 971–3363 ppm) and lower Co (114–167 ppm vs. 174–331 ppm) and Zn (<13–77 ppm vs. 35–331 ppm) contents than those from crustal peridotites. Although there is some overlap of Ni contents for the two types of peridotites, the Ni/Co ratios show a clear bimodal distribution (Fig. 4d), with mantle peridotite olivines (17–27) distinctly higher than crustal peridotite olivines (5–11). This dichotomy accords with the observation that Ni/Co ratios in olivine increase with melting degree and decrease with magma crystallization (Sobolev et al., 2007). Therefore, we suggest that the Ni/Co ratio in olivine combined with the Fo value can successfully discriminate between mantle and crustal peridotites (Fig. 4d). When mantle wedge peridotites were involved into the subduction channel, they would undergo HP–UHP metamorphism and crustal metasomatism. In the following sections, we propose to evaluate the role of olivine minor elements in monitoring these processes.

5. From hot lithospheric mantle to cool subduction zones

Re-Os isotope data indicate that the mantle-derived orogenic peridotites collected in this study were derived from ancient continental lithospheric mantle (Beyer et al., 2004; Chen et al., 2017; Su et al., 2016a). Peridotitic mineral inclusions in diamond represent a proxy for pristine continental lithospheric mantle (Stachel and Harris, 2008). As shown in Fig. 5, although olivines in orogenic mantle peridotites show slightly different compositions (lower Fo values and higher Co contents) from olivine inclusions in diamond from the Siberian, Slave and other cratons (Sobolev et al., 2009), they have nearly identical compositions to those in cratonic peridotite xenoliths. This indicates that both orogenic and cratonic mantle peridotites might be reworked to various extent after their formation.

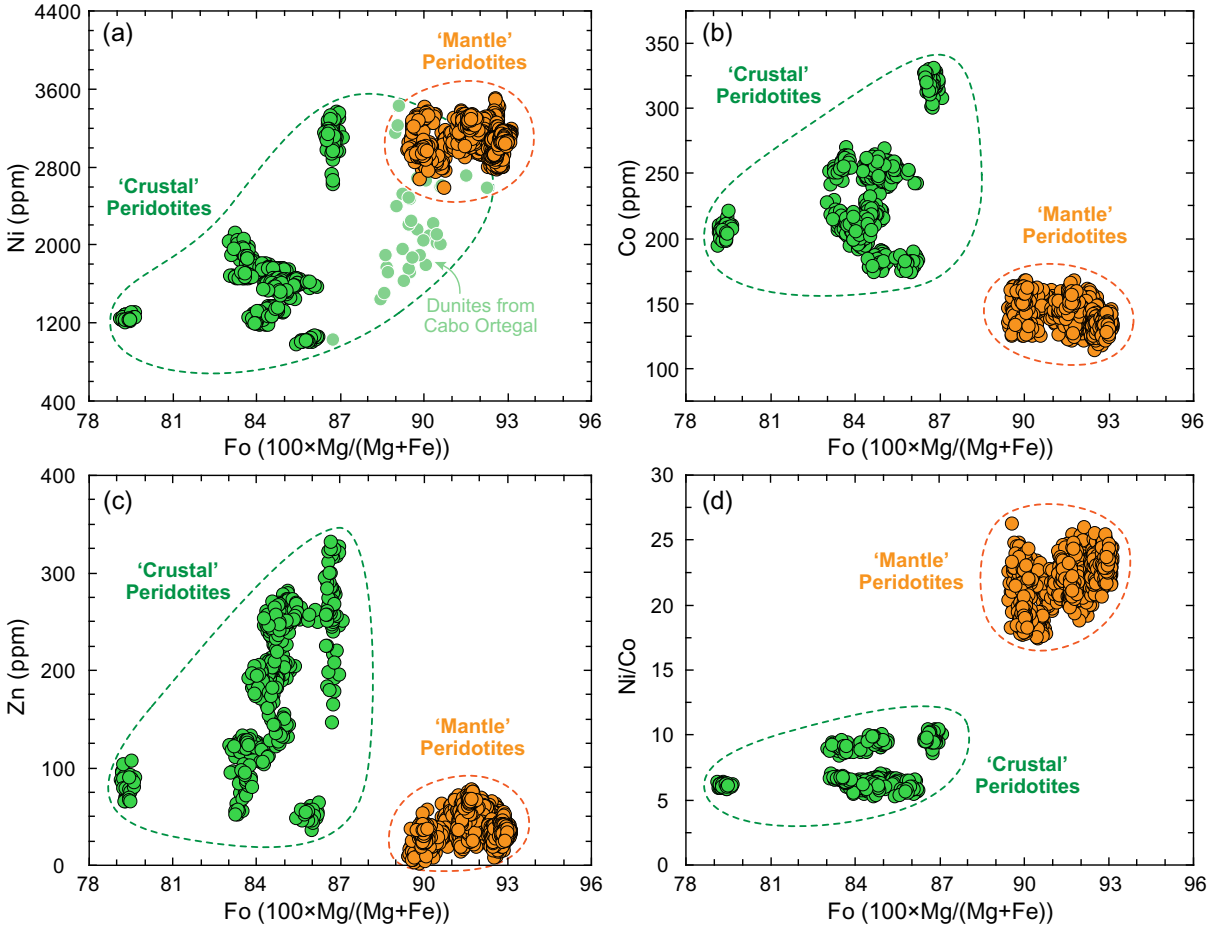

Fig. 4. Olivine chemistry for discrimination between 'mantle' and 'crustal' origins of orogenic peridotites. (a) Fo vs. Ni, (b) Fo vs. Co, (c) Fo vs. Zn and (d) Fo vs. Ni/Co. The orange and green dashed circles indicate the olivine compositional fields of orogenic mantle and crustal peridotites, respectively. The data for olivines in the Cabo Ortegal dunites are from Santos et al. (2002). (For interpretation of the references to color in this figure legend, the reader is referred to the web version of this article.)

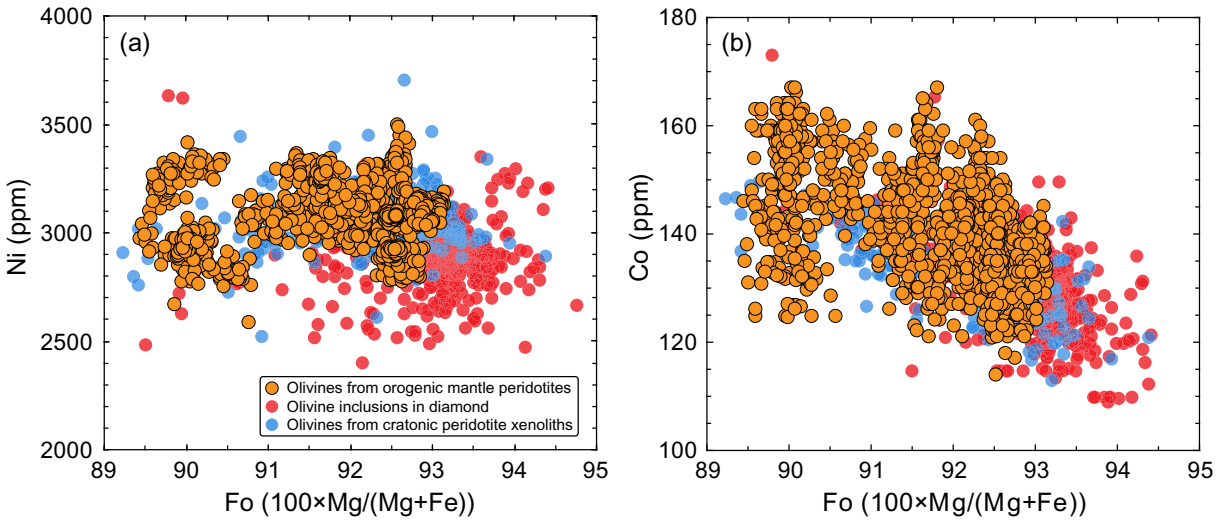

Fig. 5. Plots of Fo vs. (a) Ni and (b) Co in olivines from orogenic mantle peridotites. Also shown are data for olivine inclusions in diamond and olivines from cratonic peridotite xenoliths (Sobolev et al., 2009).

Orogenic peridotites commonly record HP–UHP metamorphism at 700–900 °C and ~2–7 GPa resulted from continental subduction (e.g., Chen et al., 2013a; Yang and Jahn, 2000; Ye et al., 2009). These *P–T* conditions reflect cold thermal structures in subduction zones (Peacock, 1995). In contrast, cratonic peridotite xenoliths and mineral inclusions in diamond have equilibrated under higher temperature conditions (800–1400 °C) at corresponding depths (Lee et al., 2011; Stachel and Harris, 2008). The question is whether minor elements in olivines can record the transfer of hot lithospheric mantle peridotites to cool subduction zones.

Temperature effects in olivine have been recognized for Ca, Al, Cr, Ti, V and Sc (De Hoog et al., 2010; Witt-Eickschen and O'Neill, 2005). A positive relationship between olivine Ti content and temperature was observed in spinel peridotites by O'Reilly et al. (1997) and was later reproduced by experimental work (Hermann et al., 2005). However, the Ti contents of olivine are also affected by bulk composition, equilibrated minerals, and OH planar defects (Hermann et al., 2005, 2007; McDonough et al., 1992). The olivine Ti contents of orogenic mantle peridotites (mostly <5–90 ppm) are comparable to those of lithospheric mantle peridotite xenoliths (predominantly 6–60 ppm; Sobolev et al., 2009), casting doubt on the reliability of Ti in olivine as a temperature indicator for orogenic peridotites. Because V and Sc in olivine are below the EPMA detection limits, we do not discuss them further. The temperature dependence of Ca, Al and Cr in olivine has been well used to construct Ca-, Al- and Cr-in-olivine thermometers based on natural peridotite compositions (De Hoog et al., 2010). The Al-in-olivine thermometer for mantle peridotites has also been experimentally calibrated by Bussweiler et al. (2017). Moreover, olivine Ca, Al and Cr contents in strongly metasomatized lherzolites (e.g., Zhimafang and Jiangzhuang) are close to or even lower than those in weakly metasomatized harzburgites/dunites (e.g., Raobazhai and Friningen) (Table 1), implying that crustal metasomatism has little influence on the Ca, Al and Cr contents of orogenic peridotite olivines.

As shown in Fig. 6, the Ca, Al and Cr contents in olivines from orogenic mantle peridotites are clearly lower than those from cratonic peridotite xenoliths and inclusions in diamond, indicating that the Ca, Al and Cr contents of orogenic peridotite olivines were successfully redistributed during subduction zone processes. Compared with Al and Cr, which are mostly below the detection limits of HP-EPMA in this study, our data on Ca contents can provide more reliable temperature estimates. Application of the Ca-in-olivine geothermometer of De Hoog et al. (2010) to orogenic mantle peridotites yields equilibration temperatures of 700–950 °C (Fig. 6a), which are consistent with the results of previous studies (700–900 °C) using Mg-Fe exchange geothermometers and thermodynamic modeling (e.g., Chen et al., 2013a; Yang and Jahn, 2000; Ye et al., 2009). Moreover, the diffusion coefficient of Ca in olivine is lower than the Mg-Fe interdiffusion coefficient (Coogan et al., 2005; Qian et al., 2010), which benefits the preservation of olivine peak Ca contents during exhumation of orogenic peridotites and thus makes the Ca-in-olivine thermometer better for recording metamorphic peak temperatures. This geothermometer can also be a good choice for orogenic dunite and harzburgite due to lack of suitable geothermometers for such highly depleted peridotites. These findings support that Ca in olivine is a useful geothermometer for orogenic peridotites and can provide valuable constraints on mantle geodynamics related to continental subduction.

6. Na-in-olivine: A potential pressure indicator for orogenic mantle peridotites

Simkin and Smith (1970) suggested that the pressure of igneous olivine crystallization plays a role in determining its Ca content. Subsequently, the pressure dependence of Ca in olivine was reported in some mantle peridotites (Finnerty and Boyd, 1978) and was later calibrated as an empirical barometer (Adams and Bishop, 1982; Köhler and Brey, 1990). However, further studies demonstrate that the temperature dependence of Ca in olivine is much greater than the pressure effect (De Hoog et al., 2010; Ford et al., 1983; O'Reilly et al., 1997). Our data also support this argument, which hampers the use of Ca in olivine as a pressure indicator for peridotites. Bodinier et al. (1987) observed a pressure dependence of Ti distribution between olivine and orthopyroxene in spinel and garnet peridotites. The occurrence of oriented ilmenite rods in olivine from the Alpe Arami peridotite massif was initially suggestive of high Ti solubility in olivine at great mantle depths (Dobrzhinetskaya et al., 1996). However, many studies have demonstrated that there is no significant increase in Ti content with pressure and that OH incorporation, bulk composition, temperature and equilibrated minerals play key roles in influencing Ti contents in mantle olivine (Hermann et al., 2005, 2007; McDonough et al., 1992; Ulmer et al., 1998). In summary, Ca and Ti in olivine cannot be used to infer pressures for orogenic peridotites.

Experimental studies have shown that the partition coefficient for Na in olivine greatly increases with pressure up to 14 GPa due to its larger ionic radius and compressibility than those of high valence cations (Imai et al., 2012; Ozawa, 1991; Taura et al., 1998). Orogenic mantle peridotites collected in this study underwent subduction

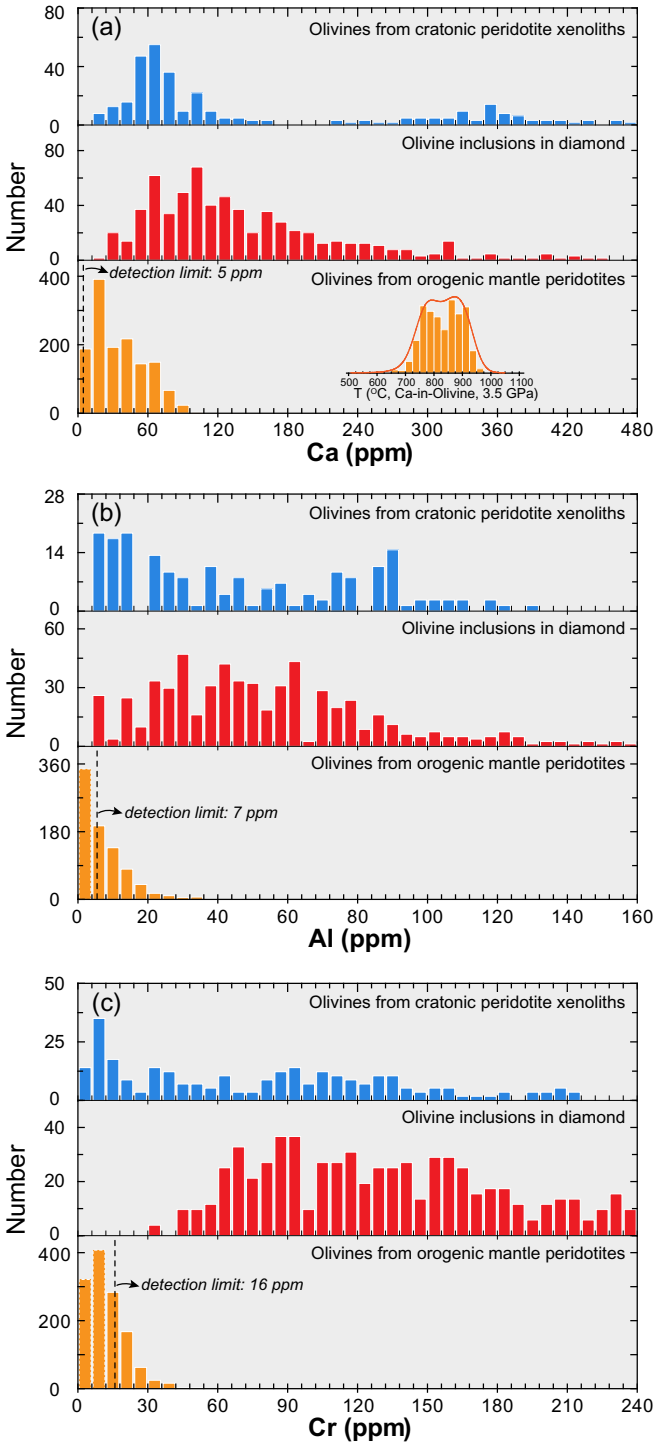

Fig. 6. Comparison of (a) calcium, (b) aluminum and (c) chromium concentrations in olivines from orogenic mantle peridotites and cratonic peridotites (xenoliths and inclusions in diamond; Sobolev et al., 2009). Most of the Al and Cr contents in olivines from orogenic mantle peridotites are below the detection limits of HP-EPMA, marked by dashed lines. Temperatures for orogenic mantle peridotites were calculated by using the Ca-in-olivine geothermometer at 3.5 GPa (De Hoog et al., 2010). A simple calculation shows that pressure has limited impact on the calculated temperatures (~50 °C/GPa) and that the pressure effect gradually diminishes with the decrease of olivine Ca contents.

metamorphism varying from ~2 to 7 GPa. Although a positive correlation between olivine Na content and temperature was observed in some high-*T* peridotite xenoliths (De Hoog et al., 2010), the studied orogenic peridotites show a narrow temperature range of 700–900 °C (e.g., Chen et al., 2013a; Yang and Jahn, 2000; Ye et al., 2009). The Raobazhai spinel peridotites record a higher metamorphic temperature of ~900 °C (Zheng et al., 2008) than most other orogenic peridotites, but their olivine Na contents are clearly lower than those in the latter (Table 1). Therefore, temperature effect on olivine Na contents is very limited for orogenic peridotites. In this regard, we can use our data to examine the possible pressure dependence of Na in olivine. For simplicity, we subdivide orogenic mantle peridotites into two groups: spinel-facies and garnet-facies peridotites. The latter are generally equilibrated at higher pressures (3.0–7.0 GPa) than the former (<~2.5 GPa). Fig. 7 illustrates that garnet-facies peridotites have overall higher olivine Na contents than spinel-facies peridotites. The olivine Na contents in garnet-facies peridotites are typically greater than ~20 ppm, whereas those in spinel-facie peridotites are mostly below the detection limit of 11 ppm (Table 1). Based on experimental work and this study, Na in olivine can be a potential pressure indicator for orogenic mantle peridotites, which deserves further investigation.

7. Metasomatism in the mantle wedge: Insights from minor elements in olivine?

Mantle wedge-derived orogenic peridotites hold abundant evidence of crustal metasomatism and thus open a window to crust–mantle interaction in subduction zones. In general, two types of metasomatism are identified in orogenic peridotites: modal and cryptic metasomatism (Chen et al., 2017; Li et al., 2016; Malaspina et al., 2006; Scambelluri et al., 2008; Zhang et al., 2011). Modal metasomatism is characterized by the occurrence of secondary minerals, such as phlogopite, Ti-clinohumite, pargasite, rutile, zircon and carbonate phases. Cryptic metasomatism results in merely changing the primary mineral compositions (mainly trace elements) without the formation of new phases. To trace cryptic metasomatism, previous studies mainly focused on garnet and clinopyroxene (e.g., Chen et al., 2013b; Zheng et al., 2005) but rarely dealt with olivine due to its relatively low trace element contents.

However, several studies have found that minor and trace elements in olivine may act as tracers of crustal metasomatism within the mantle (e.g., Foley et al., 2006, 2013; Neave et al., 2018; Prelević et al., 2013). For example, olivines from Antarctic mantle peridotite xenoliths show distinct trace element contents between cores and rims, with rims having higher concentrations of Ti, Cr, V and Zn taken from the metasomatic melt (Foley et al., 2006). Enrichment in Li in olivine has been identified as evidence of interaction with continental sediments or carbonatitic melts (Foley et al., 2013; Prelević et al., 2013). Our recent work suggests that olivines associated with carbonatitic metasomatism may show

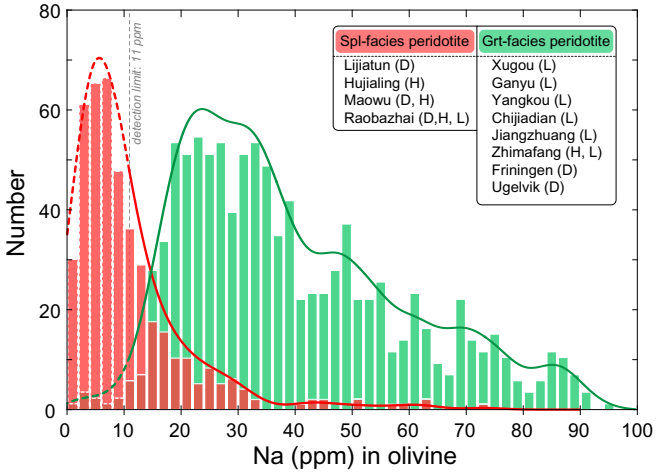

Fig. 7. Histograms of olivine Na contents showing a systematic difference between spinel-facies (red) and garnet-facies (green) orogenic mantle peridotites. The data below the detection limit (11 ppm) are marked by the dashed lines. D, dunite; H, harzburgite; L, lherzolite. (For interpretation of the references to colour in this figure legend, the reader is referred to the web version of this article.)

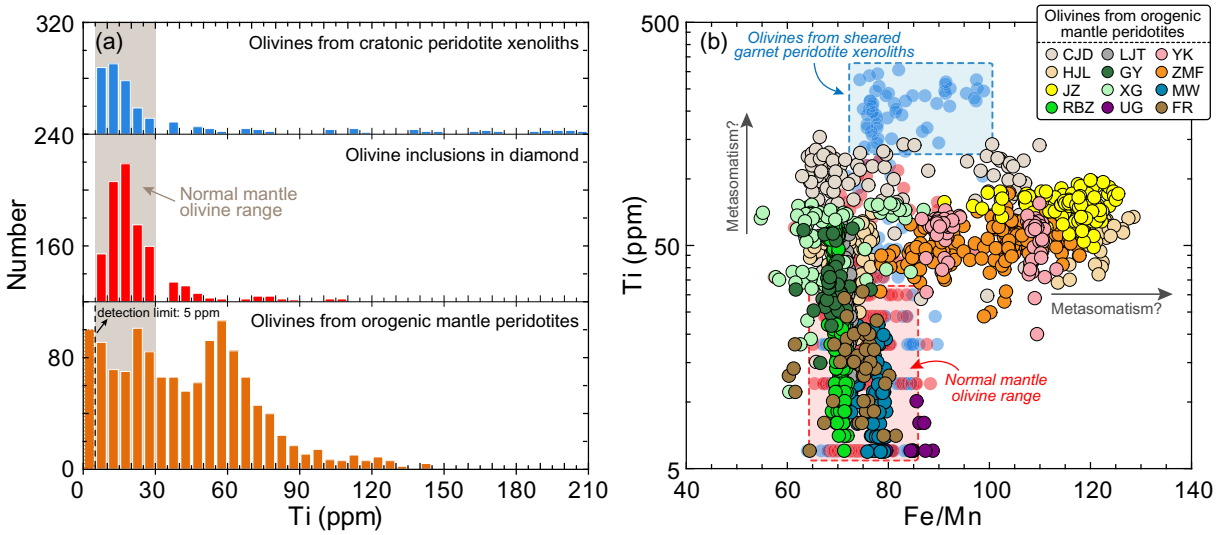

Fig. 8. (a) Comparison of Ti contents in olivines from orogenic mantle peridotites and cratonic peridotites (xenoliths and inclusions in diamond; Sobolev et al., 2009). (b) Fe/Mn ratios vs. Ti contents in olivines. The normal mantle olivine range indicates the main compositional range of olivines from cratonic peridotite xenoliths and inclusions in diamond. The sheared peridotite xenoliths experienced refertilization at the base of cratonic mantle (Sobolev et al., 2009). Abbreviation: CJD–Chijiadian; LJT–Lijiatun; YK–Yangkou; HJL–Hujialing; GY–Ganyu; ZMF–Zhimafang; JZ–Jiangzhuang; XG–Xugou; MW–Maowu; RBZ–Raobazhai; UG–Ugelvik; FR–Friningen.

higher Ca and lower Ti contents than residual olivines (Su et al., 2016a). In addition, olivines in fresh and serpentinized orogenic peridotites from the same locality (e.g., the Yangkou lherzolites and the Friningen dunites) show nearly identical minor element compositions (Table 1), indicating that olivine minor elements can overcome the influence of hydrothermal alternation and provide faithful information about crustal metasomatism in the mantle wedge.

Orogenic mantle peridotites display a uniform distribution of olivine Ti contents from <5 to ~80 ppm (Fig. 8a). In contrast, most olivines from cratonic peridotite xenoliths and inclusions in diamond exhibit a limited range of Ti contents from 5 to 30 ppm (Sobolev et al., 2009). The higher Ti contents for orogenic peridotites first rule out the role of temperature due to their cooler conditions and are more likely to result from subducted crustal metasomatism. For example, the wide occurrence of Ti-clinohumite and rutile in orogenic garnet lherzolites (e.g., Zhimafang and Jiangzhuang) reveals that the mantle wedge has been metasomatized by Ti-rich liquids (Ye et al., 2009; Zhang et al., 2011). Olivines in such strongly metasomatized lherzolites typically have higher Ti contents than those from harzburgites and dunites (e.g., Maowu, Friningen and Ugelvik) (Fig. 8b). Previous studies indicate that incorporation of Ti and OH is strongly linked to orogenic peridotite olivines and that incorporation of water (OH) in olivine is closely related to fluid metasomatism in subduction zones (Hermann et al., 2005, 2007). These results imply high sensitivity of Ti in olivine to crustal metasomatism. In addition, high-Ti olivines from orogenic peridotites have overall higher Fe/Mn ratios (Fig. 8b), similar to those from high-*T* sheared garnet peridotite xenoliths that experienced refertilization at the base of the continental lithosphere (Sobolev et al., 2009). The Mn contents in mantle olivines normally decrease with increasing partial melting (O'Reilly et al., 1997) and yield a negative correlation with Fo values (mantle melting trend in Fig. 9a). However, olivines in orogenic peridotites generally deviate from the mantle melting trend and show a wider range of Mn contents than normal mantle olivines (Sobolev et al., 2009) (Fig. 9). In particular, olivines that deviate from the mantle melting trend are

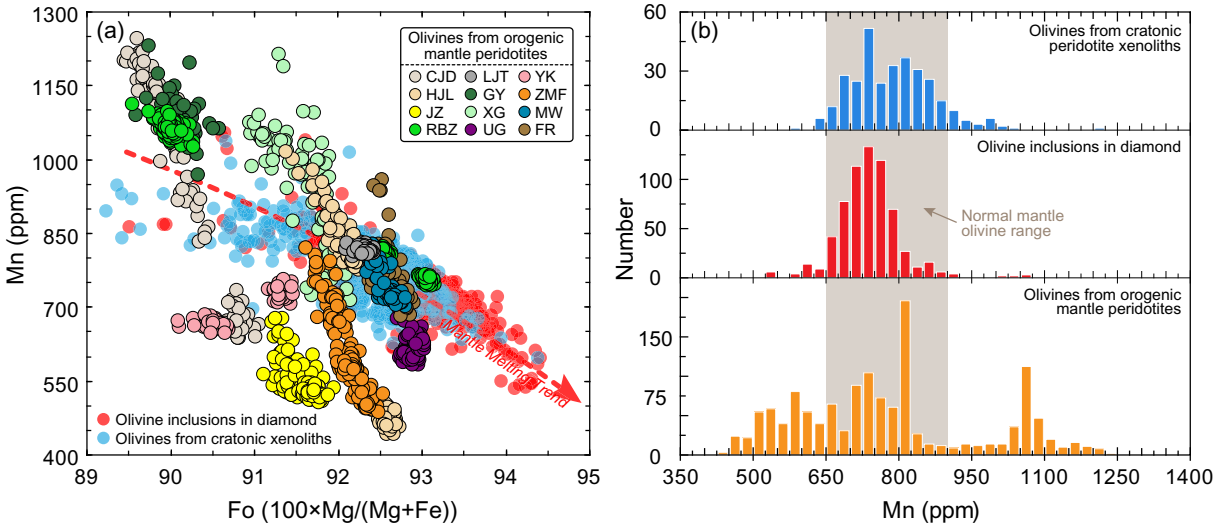

Fig. 9. (a) Relationship between Fo values and Mn contents in olivines. The red dashed line with arrow is a visual fit through the data for cratonic peridotites (red and sky blue data points) and can be treated as representing the mantle melting trend. (b) Comparison of Mn contents in olivines from orogenic mantle peridotites and cratonic peridotites (xenoliths and inclusions in diamond; Sobolev et al., 2009). (For interpretation of the references to colour in this figure legend, the reader is referred to the web version of this article.)

mostly found in strongly metasomatized lherzolites (e.g., Zhimafang, Jiangzhuang and Chijiadian), and these olivines also have high Ti contents. Experimental studies showed that the MnO contents of subducted crust-derived melts vary from 0.01 to 0.41 wt% (Hermann and Rubatto, 2009; Rapp and Watson, 1995). Given that the partition coefficient of Mn between olivine and melt is close to unity (0.77–1.09; Le Roux et al., 2011), crust–mantle interaction could therefore cause orogenic peridotite olivines to have variable Mn contents. We suggest that Ti and Mn in olivine might be helpful proxies for tracing crustal metasomatism in the mantle wedge.

8. Conclusions and outlook

We report large amounts of major and minor element data for olivines from orogenic peridotites. Olivine geochemistry has emerged as a particularly powerful tool for recognizing the nature and evolution of orogenic peridotites. The Ni/Co ratio of olivine can play a decisive role in the distinction between mantle and crustal peridotites. Ca, Al and Cr, especially Ca, in olivine are useful geothermometers for orogenic peridotites, and their low contents indicate that mantle-derived orogenic peridotites have undergone transfer from hot continental lithosphere to cool subduction zones. Na in olivine has great potential to constrain pressure conditions of orogenic mantle peridotites. Ti and Mn in olivine can provide significant information on crust–mantle interaction in subduction zones.

Our data outline several promising directions for olivine minor element geochemistry in orogenic peridotites, and further studies are needed to evaluate the behavior of trace elements (mostly <1 ppm) in olivine, such as Li, V, Sc, Cu, Zr and Y. The V/Sc ratio is increasingly used as a monitor of oxidation state (Foley et al., 2013; Lee et al., 2005), which may provide constraints on the oxygen fugacity of the sub-arc mantle. Li, Zr and Y in olivine have been involved in explaining compositional heterogeneities in the mantle (Neave et al., 2018; Prelević et al., 2013) and thus hold promise for deciphering crustal metasomatism in the mantle wedge. Given that the most Cu-rich igneous olivines are found in arc magmas (Wade et al., 2006), assessing the olivine Cu contents of mantle wedge peridotites is essential. Finally, we suggest that it will have broad prospects for investigating olivine geochemistry in the realm of subduction zone geodynamics.

Supplementary data to this article can be found online at https://doi.org/10.1016/j.lithos.2019.06.029.

Acknowledgments

We thank Profs. Xu-Ping Li and Jian-Jun Yang and Dr. Yong-Sheng Gai for providing some peridotite samples and two anonymous reviewers for their insightful reviews. This work was supported by the Chinese State Key Research and Development Program (2016YFE0203000), the National Science Foundation of China (41490614, 41802059, 41822202), the Youth Innovation Promotion Association CAS (2017090), the National Postdoctoral Program for Innovative Talents (BX201700239), and China Postdoctoral Science Foundation (2017M620065).

References

Ackerman, L., Jelínek, E., Medaris Jr., G., Ježek, J., Siebel, W., Strnad, L., 2009. Geochemistry of Fe-rich peridotites and associated pyroxenites from Horní Bory, Bohemian Massif: insights into subduction-related melt–rock reactions. Chem. Geol. 259, 152–167.

Adams, G., Bishop, F., 1982. Experimental investigation of Ca–Mg exchange between olvine, orthopyroxene, and clinopyroxene: potential for geobarometry. Earth Planet. Sci. Lett. 57, 241–250.

Beyer, E.E., Brueckner, H.K., Griffin, W.L., O'Reilly, S.Y., Graham, S., 2004. Archean mantle fragments in proterozoic crust, Western Gneiss Region, Norway. Geology 32, 609–612.

Beyer, E.E., Griffin, W.L., O'Reilly, S.Y., 2006. Transformation of Archaean lithospheric mantle by refertilization: evidence from exposed peridotites in the Western Gneiss Region, Norway. J. Petrol. 47, 1611–1636.

Bodinier, J.L., Godard, M., 2003. Orogenic, ophiolitic, and abyssal peridotites. In: Carlson, R.W. (Ed.), Treatise on Geochemistry. Mantle and Core vol. 2. Elsevier Science Ltd., pp. 103–170.

Bodinier, J.L., Dupuy, C., Dostal, J., Merlet, C., 1987. Distribution of trace transition elements in olivine and pyroxenes from ultramafic xenoliths; application of microprobe analysis. Am. Mineral. 72, 902–913.

Brueckner, H.K., Medaris, L.G., 2000. A general model for the intrusion and evolution of 'mantle' garnet peridotites in high-pressure and ultra-high-pressure metamorphic terranes. J. Metamorph. Geol. 18, 123–133.

Bussweiler, Y., Brey, G.P., Pearson, D.G., Stachel, T., Stern, R.A., Hardman, M.F., Kjarsgaard, B.A., Jackson, S.E., 2017. The aluminum-in-olivine thermometer for mantle peridotites—experimental versus empirical calibration and potential applications. Lithos 272, 301–314.

Carswell, D.A., Harvey, M.A., Al-Samman, A., 1983. The petrogenesis of contrasting Fe–Ti and Mg–Cr garnet peridotite types in the high grade gneiss complex of Western Norway. Bull. Mineral. 106, 727–750.

Chen, Y., Ye, K., Guo, S., Wu, T.F., Liu, J.B., 2013a. Multistage metamorphism of garnet orthopyroxenites from the Maowu mafic–ultramafic complex, Dabieshan UHP terrane, eastern China. Int. Geol. Rev. 55, 1239–1260.

Chen, Y., Ye, K., Wu, Y.W., Guo, S., Su, B., Liu, J.B., 2013b. Hydration and dehydration in the lower margin of a cold mantle wedge: implications for crust–mantle interactions and petrogeneses of arc magmas. Int. Geol. Rev. 55, 1506–1522.

Chen, Y., Su, B., Guo, S., 2015. The Dabie–Sulu orogenic peridotites: progress and key issues. Sci. China Earth Sci. 58, 1679–1699.

Chen, Y., Su, B., Chu, Z.Y., 2017. Modification of an ancient subcontinental lithospheric mantle by continental subduction: insight from the Maowu garnet peridotites in the Dabie UHP belt, eastern China. Lithos 278, 54–71.

Coogan, L.A., Hain, A., Stahl, S., Chakraborty, S., 2005. Experimental determination of the diffusion coefficient for calcium in olivine between 900 °C and 1500 °C. Geochim. Cosmochim. Acta 69, 3683–3694.

Coogan, L.A., Saunders, A.D., Wilson, R., 2014. Aluminum-in-olivine thermometry of primitive basalts: evidence of an anomalously hot mantle source for large igneous provinces. Chem. Geol. 368, 1–10.

De Hoog, J.C.M., Gall, L., Cornell, D.H., 2010. Trace-element geochemistry of mantle olivine and application to mantle petrogenesis and geothermobarometry. Chem. Geol. 270, 196–215.

Dobrzhinetskaya, L., Green, H.W., Wang, S., 1996. Alpe Arami: a peridotite massif from depths of more than 300 kilometers. Science 271, 1841–1845.

Finnerty, A., Boyd, F.R., 1978. Pressure-Dependent Solubility of Calcium in Forsterite Coexisting with Diopside and Enstatite. vol. 77. Carnegie Institution of Washington, pp. 713–717.

Foley, S.F., Andronikov, A.V., Jacob, D.E., Melzer, S., 2006. Evidence from Antarctic mantle peridotite xenoliths for changes in mineralogy, geochemistry and geothermal gradients beneath a developing rift. Geochim. Cosmochim. Acta 70, 3096–3120.

Foley, S.F., Prelevic, D., Rehfeldt, T., Jacob, D.E., 2013. Minor and trace elements in olivines as probes into early igneous and mantle melting processes. Earth Planet. Sci. Lett. 363, 181–191.

Ford, C.E., Russell, D.G., Craven, J.A., Fisk, M.R., 1983. Olivine–liquid equilibria: temperature, pressure and composition dependence of the crystal/liquid cation partition coefficient for Mg, Fe^{2+}, Ca and Mn. J. Petrol. 24, 256–265.

Gai, Y.S., Liu, L., Wang, C., Yang, W.Q., Kang, L., Cao, Y.T., Liao, X.Y., 2017. Discovery of coesite in eclogite from Keqike Jianggalesayi: new evidence for ultrahigh-pressure metamorphism in South Altyn Tagh, Northwestern China. Sci. Bull. 62, 1048–1051.

Gee, D.G., Janák, M., Majka, J., Robinson, P., van Roermund, H., 2013. Subduction along and within the Baltoscandian margin during closing of the Iapetus Ocean and Baltica-Laurentia collision. Lithosphere 5, 169–178.

Hermann, J., Rubatto, D., 2009. Accessory phase control on the trace element signature of sediment melts in subduction zones. Chem. Geol. 265, 512–526.

Hermann, J., O'Neill, H.S.C., Berry, A.J., 2005. Titanium solubility in olivine in the system TiO_2–MgO–SiO_2: no evidence for an ultra-deep origin of Ti-bearing olivine. Contrib. Mineral. Petrol. 148, 746–760.

Hermann, J., Gerald, J.D.F., Malaspina, N., Berry, A.J., Scambelluri, M., 2007. OH-bearing planar defects in olivine produced by the breakdown of Ti-rich humite minerals from Dabie Shan (China). Contrib. Mineral. Petrol. 153, 417–428.

Hervig, R., Smith, J., Dawson, J., 1986. Lherzolite xenoliths in kimberlites and basalts: petrogenetic and crystallochemical significance of some minor and trace elements in olivine, pyroxenes, garnet and spinel. Earth Environ. Sci. Trans. R. Soc. Edinb. 77, 181–201.

Imai, T., Takahashi, E., Suzuki, T., Hirata, T., 2012. Element partitioning between olivine and melt up to 10 GPa: implications for the effect of pressure. Phys. Earth Planet. Inter. 212, 64–75.

Köhler, T.P., Brey, G.P., 1990. Calcium exchange between olivine and clinopyroxene calibrated as a geothermobarometer for natural peridotites from 2 to 60 kb with applications. Geochim. Cosmochim. Acta 54, 2375–2388.

Le Roux, V., Dasgupta, R., Lee, C.T.A., 2011. Mineralogical heterogeneities in the Earth's mantle: constraints from Mn, Co, Ni and Zn partitioning during partial melting. Earth Planet. Sci. Lett. 307, 395–408.

Lee, C.T.A., Leeman, W.P., Canil, D., Li, Z.X.A., 2005. Similar V/Sc systematics in MORB and arc basalts: Implications for the oxygen fugacities of their mantle source regions. J. Petrol. 46, 2313–2336.

Lee, C.T.A., Luffi, P., Chin, E.J., 2011. Building and destroying continental mantle. Annu. Rev. Earth Planet. Sci. 39, 59–90.

Lenoir, X., Garrido, C.J., Bodinier, J.L., Dautria, J.M., Gervilla, F., 2001. The recrystallization front of the ronda peridotite: evidence for melting and thermal erosion of subcontinental lithospheric mantle beneath the Alboran Basin. J. Petrol. 42, 141–158.

Li, X.P., Yang, J.S., Robinson, P., Xu, Z.Q., Li, T.F., 2011. Petrology and geochemistry of UHP-metamorphosed ultramafic–mafic rocks from the main hole of the Chinese Continental Scientific Drilling Project (CCSD-MH), China: fluid/melt–rock interaction: mafic–ultramafic complex from CCSD-MH. J. Asian Earth Sci. 42, 661–683.
Li, H.Y., Chen, R.X., Zheng, Y.F., Hu, Z.C., 2016. The crust–mantle interaction in continental subduction channels: zircon evidence from orogenic peridotite in the Sulu orogen. J. Geophys. Res. Solid Earth 121, 687–712.
Liu, L., Sun, Y., Xiao, P., Che, Z., Luo, J., Chen, D., Wang, Y., Zhang, A., Chen, L., Wang, Y., 2002. Discovery of ultrahighpressure magnesite-bearing garnet lherzolite (>3.8 GPa) in the Altyn Tagh, Northwest China. Chin. Sci. Bull. 47, 881–886.
Malaspina, N., Hermann, J., Scambelluri, M., Compagnoni, R., 2006. Polyphase inclusions in garnet-orthopyroxenite (Dabie Shan, China) as monitors for metasomatism and fluid-related trace element transfer in subduction zone peridotite. Earth Planet. Sci. Lett. 249, 173–187.
McDonough, W., Stosch, H.G., Ware, N., 1992. Distribution of titanium and the rare earth elements between peridotitic minerals. Contrib. Mineral. Petrol. 110, 321–328.
Medaris, J.L.G., Carswell, D.A., 1990. Petrogenesis of Mg–Cr garnet peridotites in European metamorphic belts. Eclogite Facies Rocks 260–290.
Neave, D.A., Shorttle, O., Oeser, M., Weyer, S., Kobayashi, K., 2018. Mantle-derived trace element variability in olivines and their melt inclusions. Earth Planet. Sci. Lett. 483, 90–104.
O'Reilly, S.Y., Chen, D., Griffin, W., Ryan, C., 1997. Minor elements in olivine from spinel lherzolite xenoliths: implications for thermobarometry. Mineral. Mag. 61, 257–269.
Ozawa, S., 1991. Trivalent Cations in Olivine and their Implication to the Upper Mantle Tectonics as Inferred from the High Pressure Experiments. Doctoral thesis. The University of Tokyo.
Peacock, S.M., 1995. Ultrahigh-pressure metamorphic rocks and the thermal evolution of continent collision belts. Island Arc 4, 376–383.
Prelević, D., Jacob, D.E., Foley, S.F., 2013. Recycling plus: a new recipe for the formation of Alpine–Himalayan orogenic mantle lithosphere. Earth Planet. Sci. Lett. 362, 187–197.
Qian, Q., O'Neill, H.S.C., Hermann, J., 2010. Comparative diffusion coefficients of major and trace elements in olivine at ~950 °C from a xenocryst included in dioritic magma. Geology 38, 331–334.
Rapp, R.P., Watson, E.B., 1995. Dehydration melting of metabasalt at 8–32 kbar: implications for continental growth and crust–mantle recycling. J. Petrol. 36, 891–931.
Reverdatto, V.V., Selyatitskiy, A.Y., Carswell, D.A., 2008. Geochemical distinctions between "crustal" and mantle-derived peridotites/pyroxenites in high/ultrahigh pressure metamorphic complexes. Russ. Geol. Geophys. 49, 73–90.
Santos, J., Schärer, U., Gil Ibarguchi, J.I., Girardeau, J., 2002. Genesis of pyroxenite-rich peridotite at Cabo Ortegal (NW Spain): geochemical and Pb–Sr–Nd isotope data. J. Petrol. 43, 17–43.
Scambelluri, M., Pettke, T., van Roermund, H.L.M., 2008. Majoritic garnets monitor deep subduction fluid flow and mantle dynamics. Geology 36, 59–62.
Simkin, T., Smith, J., 1970. Minor-element distribution in olivine. J. Geol. 78, 304–325.
Smith, D.C., 1984. Coesite in clinopyroxene in the caledonides and its implications for geodynamics. Nature 310, 641–644.
Sobolev, A.V., Hofmann, A.W., Sobolev, S.V., Nikogosian, I.K., 2005. An olivine-free mantle source of Hawaiian shield basalts. Nature 434, 590–597.
Sobolev, A.V., Hofmann, A.W., Kuzmin, D.V., Yaxley, G.M., Arndt, N.T., Chung, S.L., Danyushevsky, L.V., Elliott, T., Frey, F.A., Garcia, M.O., Gurenko, A.A., Kamenetsky, V.S., Kerr, A., Krivolutskaya, N., Matvienkov, V., Nikogosian, I.K., Rocholl, A., Sigurdsson, I.A., Sushchevskaya, N.M., Teklay, M., 2007. The amount of recycled crust in sources of mantle-derived melts. Science 316, 412–417.
Sobolev, N.V., Logvinova, A.M., Zedgenizov, D.A., Pokhilenko, N.P., Malygina, E.V., Kuzmin, D.V., Sobolev, A.V., 2009. Petrogenetic significance of minor elements in olivines from diamonds and peridotite xenoliths from kimberlites of Yakutia. Lithos 112, 701–713.
Song, S.G., Su, L., Niu, Y.L., Zhang, L.F., Zhang, G.B., 2007. Petrological and geochemical constraints on the origin of garnet peridotite in the North Qaidam ultrahigh-pressure metamorphic belt, northwestern China. Lithos 96, 243–265.
Spengler, D., van Roermund, H.L.M., Drury, M.R., Ottolini, L., Mason, P.R., Davies, G.R., 2006. Deep origin and hot melting of an Archaean orogenic peridotite massif in Norway. Nature 440, 913–917.
Stachel, T., Harris, J.W., 2008. The origin of cratonic diamonds—constraints from mineral inclusions. Ore Geol. Rev. 34, 5–32.
Straub, S.M., LaGatta, A.B., Martin-Del Pozzo, A.L., Langmuir, C.H., 2008. Evidence from high-Ni olivines for a hybridized peridotite/pyroxenite source for orogenic andesites from the central Mexican Volcanic Belt. Geochem. Geophys. Geosyst. 9, Q03007. https://doi.org/10.1029/2007GC001583.
Su, B., Chen, Y., Guo, S., Chu, Z.Y., Liu, J.B., Gao, Y.J., 2016a. Carbonatitic metasomatism in orogenic dunites from Lijiatun in the Sulu UHP terrane, eastern China. Lithos 262, 266–284.
Su, B., Chen, Y., Guo, S., Liu, J.B., 2016b. Origins of orogenic dunites: petrology, geochemistry, and implications. Gondwana Res. 29, 41–59.
Taura, H., Yurimoto, H., Kurita, K., Sueno, S., 1998. Pressure dependence on partition coefficients for trace elements between olivine and the coexisting melts. Phys. Chem. Miner. 25, 469–484.
Ulmer, P., Risold, A.C., Trommsdorff, V., 1998. TiO_2 solubility in mantle olivine as a function of pressure, temperature, $a(SiO_2)$, and $f(H_2)$. EOS Trans Am Geophys Union: Fall Metting Supplement. vol.79 Abstrast V12A-06.
van Roermund, H.L.M., Drury, M.R., 1998. Ultra-high pressure (P > 6 GPa) garnet peridotites in Western Norway: exhumation of mantle rocks from >185 km depth. Terra Nova 10, 295–301.
Vrijmoed, J., Austrheim, H., John, T., Hin, R., Corfu, F., Davies, G., 2013. Metasomatism in the ultrahigh-pressure Svartberget garnet-peridotite (Western Gneiss Region, Norway): implications for the transport of crust-derived fluids within the mantle. J. Petrol. 54, 1815–1848.
Wade, J.A., Plank, T., Melson, W.G., Soto, G.J., Hauri, E.H., 2006. The volatile content of magmas from Arenal volcano, Costa Rica. J. Volcanol. Geotherm. Res. 157, 94–120.
Witt-Eickschen, G., O'Neill, H.S.C., 2005. The effect of temperature on the equilibrium distribution of trace elements between clinopyroxene, orthopyroxene, olivine and spinel in upper mantle peridotite. Chem. Geol. 221, 65–101.
Xu, S., Su, W., Liu, Y., Jiang, L., Ji, S., Okay, A., Sengör, A., 1992. Diamond from the Dabie Shan metamorphic rocks and its implication for tectonic setting. Science 256, 80–82.
Xu, W.L., Yang, D.B., Gao, S., Pei, F.P., Yu, Y., 2010. Geochemistry of peridotite xenoliths in Early Cretaceous high-Mg# diorites from the central orogenic block of the North China craton: the nature of Mesozoic lithospheric mantle and constraints on lithospheric mantle. Chem. Geol. 270, 257–273.
Yang, J.J., Jahn, B.M., 2000. Deep subduction of mantle-derived garnet peridotities from the SuLu UHP metamorphic terrane in China. J. Metamorph. Geol. 18, 167–180.
Ye, K., Yao, Y., Katayama, I., Cong, B., Wang, Q., Maruyama, S., 2000. Large areal extent of ultrahigh-pressure metamorphism in the Sulu ultrahigh-pressure terrane of East China: new implications from coesite and omphacite inclusions in zircon of granitic gneiss. Lithos 52, 157–164.
Ye, K., Song, Y.R., Chen, Y., Xu, H.J., Liu, J.B., Sun, M., 2009. Multistage metamorphism of orogenic garnet-lherzolite from Zhimafang, Sulu UHP terrane, E. China: implications for mantle wedge convection during progressive oceanic and continental subduction. Lithos 109, 155–175.
Zhang, R.Y., Liou, J.G., Yang, J.S., Yui, T.F., 2000. Petrochemical constraints for dual origin of garnet peridotites from the Dabie–Sulu UHP terrane, eastern–central China. J. Metamorph. Geol. 18, 149–166.
Zhang, R.Y., Liou, J.G., Ernst, W.G., 2009. The Dabie–Sulu continental collision zone: a comprehensive review. Gondwana Res. 16, 1–26.
Zhang, Z.M., Dong, X., Liou, J., Liu, F., Wang, W., Yui, F., 2011. Metasomatism of garnet peridotite from Jiangzhuang, southern Sulu UHP belt: constraints on the interactions between crust and mantle rocks during subduction of continental lithosphere. J. Metamorph. Geol. 29, 917–937.
Zheng, Y.F., 2012. Metamorphic chemical geodynamics in continental subduction zones. Chem. Geol. 328, 5–48.
Zheng, J.P., Zhang, R.Y., Griffin, W., Liou, J., O'Reilly, S.Y., 2005. Heterogeneous and metasomatized mantle recorded by trace elements in minerals of the Donghai garnet peridotites, Sulu UHP terrane, China. Chem. Geol. 221, 243–259.
Zheng, J.P., Sun, M., Griffin, W.L., Zhou, M., Zhao, G., Robinson, P., Tang, H., Zhang, Z., 2008. Age and geochemistry of contrasting peridotite types in the Dabie UHP belt, eastern China: petrogenetic and geodynamic implications. Chem. Geol. 247, 282–304.
Zheng, J.P., Tang, H., Xiong, Q., Griffin, W., O'Reilly, S., Pearson, N., Zhao, J., Wu, Y., Zhang, J., Liu, Y., 2014. Linking continental deep subduction with destruction of a cratonic margin: strongly reworked North China SCLM intruded in the Triassic Sulu UHP belt. Contrib. Mineral. Petrol. 168, 1–21.